sustainability

IMPACT FACTOR 3.3

CITESCORE 6.8

Article

Experimental Comparison of Two Main Paradigms for Day-Ahead Average Carbon Intensity Forecasting in Power Grids: A Case Study in Australia

Bowen Zhang, Hongda Tian, Adam Berry, Hao Huang and A. Craig Roussac

MDPI

https://doi.org/10.3390/su16198580

sustainability

MDPI

Article

Experimental Comparison of Two Main Paradigms for Day-Ahead Average Carbon Intensity Forecasting in Power Grids: A Case Study in Australia

Bowen Zhang [1], Hongda Tian [1,*], Adam Berry [1], Hao Huang [2] and A. Craig Roussac [2]

[1] Data Science Institute, Faculty of Engineering and Information Technology, University of Technology Sydney, Ultimo, NSW 2007, Australia; bowen.zhang@student.uts.edu.au (B.Z.); adam.berry@uts.edu.au (A.B.)
[2] Buildings Alive Pty Ltd., Sydney, NSW 2000, Australia; hhuang@buildingsalive.com (H.H.); croussac@buildingsalive.com (A.C.R.)
* Correspondence: hongda.tian@uts.edu.au

Abstract: Accurate carbon intensity forecasts enable consumers to adjust their electricity use, reducing it during high fossil-fuel generation and increasing it when renewables dominate. Existing methods for carbon intensity forecasting can be categorized into a source-disaggregated approach (SDA), focused on delivering individual generation forecasts for each potential source (e.g., wind, brown-coal, etc.), and a source-aggregated approach (SAA), attempting to produce a single carbon intensity forecast for the entire system. This research aims to conduct a thorough comparison between SDA and SAA for carbon intensity forecasting, investigating the factors that contribute to variations in performance across two distinct real-world generation scenarios. By employing contemporary machine learning time-series forecasting models, and analyzing data from representative locations with varying fuel mixes and renewable penetration levels, this study provides insights into the key factors that differentiate the performance of each approach in a real-world setting. The results indicate the SAA proves to be more advantageous in scenarios involving increased renewable energy generation, with greater proportions and instances when renewable energy generation faces curtailment or atypical/peaking generation is brought online. While the SDA offers better model interpretability and outperforms in scenarios with increased niche energy generation types, in our experiments, it struggles to produce accurate forecasts when renewable outputs approach zero.

Keywords: grid carbon intensity forecasting; grid energy generation forecasting; deep learning; long short-term memory model; source-aggregated approach; source-disaggregated approach

Citation: Zhang, B.; Tian, H.; Berry, A.; Huang, H.; Roussac, A.C. Experimental Comparison of Two Main Paradigms for Day-Ahead Average Carbon Intensity Forecasting in Power Grids: A Case Study in Australia. *Sustainability* **2024**, *16*, 8580. https://doi.org/10.3390/su16198580

Academic Editor: Bowen Zhou

Received: 23 August 2024
Revised: 25 September 2024
Accepted: 29 September 2024
Published: 2 October 2024

1. Introduction

Modern human society is responsible for global warming and CO_2 emissions [1]. Electricity generation accounts for the majority of global carbon emissions, representing around 40% of total emissions in 2022, as outlined by the International Energy Agency (IEA) [2]. According to the Paris Agreement [3], the majority of countries have committed to reducing carbon emissions by around 26–28% with regard to 2005 levels by 2030, as stated in their nationally determined contributions (NDCs) report [4]. Transitioning to renewable energy sources and improving energy efficiency are among the commonly adopted measures to reduce carbon emissions outlined in NDCs [4].

While renewable generation is being increasingly integrated into modern electricity networks [5], it is seldom the sole source of power production. As a result of this partial penetration and the stochasticity of renewable energy sources, the carbon intensity of the grid will vary over time.

If we can reliably forecast grid carbon intensity factor (CIF), we can enable consumers to respond, potentially shifting their electricity consumption from periods of high CIF

to times when emissions are forecast to be low (e.g., by capitalizing on pre-cooling for buildings or by optimally deploying on-site battery charge and discharge cycles).

Despite its importance, CIF forecasting remains a complex challenge, particularly as fuel types diversify, renewable penetration increases, and energy market dynamics (and the associated energy system operational decision-making) evolve. Existing works on forecasting the CIF of the grid can be divided into two categories: a source-disaggregated approach (SDA) [6,7] and a source-aggregated approach (SAA) [8–17]. The SDA involves initially predicting the different types of energy generation and then aggregating them to calculate the CIF based on the emission factors for each generation type, while the SAA looks to produce a CIF forecast for the system as a whole directly. The benefit of the SDA is greater clarity into the contribution of individual sources to overall system CIF, while the SAA (particularly when fused with machine learning across large datasets) is well placed to capture complex system-level dynamics (e.g., non-linear relationships among environmental, market, and load conditions).

To date, there have been no studies actively comparing the performance of SDA and SAA approaches using real-world energy data, nor any exploration of how renewable penetration levels and generation types impact the relative performance of each approach. The upshot is that there is little guidance for practitioners looking to understand when and where to adopt each approach and the relative benefits of each. There has also been little research into whether and how wholesale price and grid demand impacts relative performance and model behavior. In countries like Australia and the United Kingdom, where price and demand drives generator decision-making, this is an oversight [18,19].

The key contribution of this research is to provide the first direct comparison of SDA and SAA across distinct real-world operational contexts, exploring if and how the performance and value changes for each approach. The intent is to provide initial evidence-based guidance on model framework selection to those looking to deliver practical carbon intensity forecasts. This will be achieved by utilizing modern machine learning model implementations that incorporate data collected from representative locations with different types of fuel mixes and penetration levels, and by conducting a comprehensive analysis of the key factors that differentiate the performance of each approach.

We will leverage the deep learning model to predict the CIF for both the SDA and SAA, due to its ability to capture complex patterns and non-linear relationships in large amounts of multivariate time series data [20]. This allows for an investigation of performance differences with the core model being held steady. The Long Short-Term Memory (LSTM) model, which is a state-of-the-art technique for capturing and modeling long-term dependencies and patterns within the data, such as trends, seasonality, and other complex patterns, has been selected for this purpose [21].

In order to evaluate the performance of each approach in different operational contexts, we examine the electricity supply in two Australian states with sharply distinct generation mixes: New South Wales (NSW) and South Australia (SA). NSW is a state in the region of south-eastern Australia, and is its most populous state. A significant portion of its electricity is generated from non-renewable source types, which accounted for 77.2% throughout 2022, with coal accounting for the majority of that generation. SA, in the southern central region of Australia, has a significant portion of its electricity is generated from renewable sources, including wind and solar power, which made up 64.8% throughout 2022.

The structure of this article is as follows: Section 2 presents a review of relevant studies. Section 3 provides details of the two approaches. The experiments along with discussions are given in Section 4. Lastly, the conclusions and future work are presented in Section 5.

2. Literature Review

The potential for reducing CO_2 emissions through analysis of hourly patterns of CO_2 emissions from electricity sources was shown in a case study [22] conducted in Singapore. There are several earlier studies investigating different types of carbon emission forecasting, such as the prediction of CO_2 emissions [23–28] and fluxes [29], and the prediction of

carbon emissions from fuel combustion [30]. While these studies focus more on general CO_2 emission forecasting, often considering factors such as economic and social influences, we concentrate solely on data-driven prediction approaches for grid-level CIF forecasting.

There are mainly two types of CIF: marginal and average CIF. The marginal carbon emissions rate is the rate at which the emissions change due to adjustments in the electrical load at a certain time, while the grid average carbon emission refers to the total emissions across the whole grid [31]. Anika et al. [31] compared the average and marginal carbon intensity, and revealed the importance of those two concepts. Machine learning on historical data to forecast the grid marginal CIF was utilized by studies [9,32]. The marginal CIF is highly dependent on the dispatch order and the availability of generators. As our goal is to forecast the overall carbon intensity of the electricity mix for any given time interval (e.g., an hour), we will focus on the prediction of the grid average CIF.

The average CIF refers to how many grams of CO_2-eq is released to produce a kilowatt hour (kWh) of electricity across a given time interval [33]. The definition of the grid average CIF is shown as follows:

$$\mathrm{CIF}_{\mathrm{avg},t} = \frac{\sum(E_{s,t} \times C_{s,t})}{\sum E_{s,t}} \quad (1)$$

where $CIF_{\mathrm{avg},t}$ represents the average CIF at time interval t. The electricity generated by each source type s is denoted by $E_{s,t}$. $C_{s,t}$ represents the emission rate for each type of source.

The methods to forecast the CIF can be classified into two categories: SDA and SAA. The main architecture of the SDA is to first forecast the individual generation from each renewable fuel type (e.g., wind, solar, and hydro) and non-renewable fuel type (e.g., gas and coal), and then combine them to calculate the CIF based on emission factors with Equation (1). Diptyaroop et al. [6] predicted day-ahead hourly average carbon emissions using the SDA. The Artificial Neural Network (ANN) model was applied to forecast electricity generated by each power source. Weather forecasting and time features as input variables were considered in the ANN model to extract the trends and seasonality in the data. This method was assessed using actual power generation data, and attained an average Mean Absolute Percentage Error (MAPE) of 6.4% across Europe and the US. However, some regions with high renewable energy penetration, such as Germany, exhibited greater errors, with a MAPE of 9.08%. In 2022, Diptyaroop et al. [7] proposed a similar method to [6] to forecast the grid average carbon intensity. With historical generation and weather variable data inputs, the deep learning model Convolutional Neural Network with Long Short-Term Memory combination (CNN-LSTM) was used to generate 4-day-ahead carbon intensity forecasts, which achieved a 9.78% MAPE across 13 geographically distributed regions over the 96 h forecasting period with hourly intervals.

The SAA, with its focus on system-level dynamics and the aggregation of all generators, provides a single CIF forecast for the entire system. Early studies in this space relied on the Autoregressive Integrated Moving Average (ARIMA) model [8–10]. ARIMA has known limitations with respect to capturing the types of complex non-linear relationships that are likely to exist in grid carbon intensity forecasting over time. As such, more recent studies have turned their attention to deep learning, particularly LSTMs [11,13–15] and hybrid models [12], for CIF forecasting.

Gordon [8] utilized ARIMA models and a non-linear ANN to predict cyclical changes in day-ahead CIF for the UK electricity grid, aiding in the reduction of carbon emissions by optimizing Heating, Ventilation, and Air Conditioning (HVAC) loads. Kenneth et al. [9] developed a feature selection method combined with LASSO regression and an ARIMA residual correction method to predict the CIF in the European power industry, selecting key variables to improve the prediction accuracy. Neeraj et al. [10] employed decomposition methods and ARIMA for CIF forecasting, considering the impact of market bidding. Talysson et al. [16] present a method for CIF forecasting in multi-source power generation systems using Evolving Dynamic Bayesian Networks, which adapts to incoming data by updating the network structure based on an analytical threshold. Adrian et al. [17] apply

random forest and gradient boosting models for short-term forecasting of the German generation-based CIF. Recent research [11,13–15] has confirmed the effectiveness of LSTM models in CIF forecasting across various applications. Carolina et al. [13] explored the use of an LSTM model to predict the day-ahead average CIF for electricity consumption in smart homes, finding it more accurate than traditional regression methods. Cai et al. [15] presented a day-ahead carbon emission prediction model using LSTM to forecast node carbon emission factors in a regional grid, enhancing both the environmental friendliness and the power quality. Vahid et al. [11] compared models such as Extremely Randomized Trees (ERTs), LSTM, and Extreme Learning Machines (ELMs) for predicting the day-ahead regional emissions intensity in Australia, finding that LSTM and ERT showed reasonable accuracy, while Bo et al. [14] confirmed the superiority of LSTM over other deep learning models like ANNs and Recurrent Neural Networks (RNNs) in forecasting the average CIF. Zhang et al. [12] also introduced a Graph Neural Network (GNN)-LSTM hybrid model to enhance CIF forecasting accuracy in cross-border power grids by accounting for spatial and temporal dependencies. We are following their lead in our work by also adopting LSTMs as our core model to enable comparisons between SDA and SAA.

It should be noted that, unlike previous studies, our focus is not on improving the accuracy of the average CIF forecasting through the development of various methods and models. Instead, the main objective of our research is to enhance the understanding about the factors from environmental, market, and system domains that influence the performance of SAA and SDA, and to explore their implications for future designs and applications. This research aims to move beyond conventional summaries of performance and delve deeper into the relative strengths and weaknesses of each approach.

3. Methodology

In this section, we first provide an overview of the LSTM model, including the definition and application of LSTM in our research. Subsequently, we present a detailed description about the implementations of both SAA and SDA.

3.1. LSTM Model

A deep feed-forward neural network (DFFNN), commonly referred to as a multi-layer neural network, is an architecture widely used in the field of artificial neural networks. This network can deal well with large-scale time-series data and provide accurate time-series predictions, unlike single-layer neural networks [34]. The structure of a DFFNN consists of an input layer, multiple hidden layers, and an output layer. Each hidden layer is composed of a certain number of neurons, or nodes, to be determined. Each neuron receives inputs from neurons in the previous layer, and determines weights and activation for neurons in the next layer. The weights are calculated during the training period of the neural network. The node activation function, such as the rectified linear unit and sigmoid function, is also known as the "transfer function", which is used to calculate the output of a neuron. This procedure is reiterated, and the desired outputs can be processed to the neurons in the output layer.

The architecture of DFFNN serves as a foundation for various advanced neural network models, such as the LSTM model. LSTM is a type of artificial neural network, capable of retaining a long-term memory and using it to learn patterns in long sequences of data. LSTM, with three types of gates (namely forget gates, update gates, and output gates), can deal with the gradient vanishing and exploding problem [21]. In detail, this model determines whether past information is retained or forgotten. If a value in a forget gate is close to 0, this model will forget past information with this value, whereas a value close to 1 means that it remains. An update gate, also called an input gate, is in charge of updating new information in the memory state. Afterward, an output gate decides what needs to be the input of the next hidden unit.

When designing the LSTM model, careful consideration must be given to various hyper-parameters, such as the number of neurons, the number of layers, and the activation

function, as they significantly impact its performance. Determining the optimal values for these hyper-parameters is essential to achieve the desired performance and prevent issues such as overfitting or under-fitting [35]. Overfitting problems, which result in lower performance on unseen data, can arise from a more complex neural network than necessary [36]. To address this, a grid search was conducted during the design phase of the LSTM model to identify the best hyper-parameter configurations.

LSTM, being a state-of-the-art model, is well-suited to process large-scale datasets, and can be effectively utilized in multivariate time series forecasting applications. The neural networks within LSTM exhibit the capability to capture complex patterns and effectively filter out noise. The LSTM model and hybrid models have been leveraged and proven to be more effective compared to other deep learning models for CIF forecasting in recent studies [7,11–14]. As a result, we utilized LSTM in our SAA and SDA implementations for average CIF forecasting.

The architecture of the proposed LSTM model is presented in Figure 1. Each input feature is divided into 24 h sliding windows with a 1 h moving window. These sliding windows with input features are then fed as input to the LSTM model for training. The following 24 h label windows from the training set serve as the supervised labels for the model. The hidden layers of the LSTM are designed to minimize the difference between the supervised labels and the predicted labels generated by the output layers. This learning process involves capturing and understanding the temporal dependencies within the input data, enabling the model to make accurate predictions based on the given inputs.

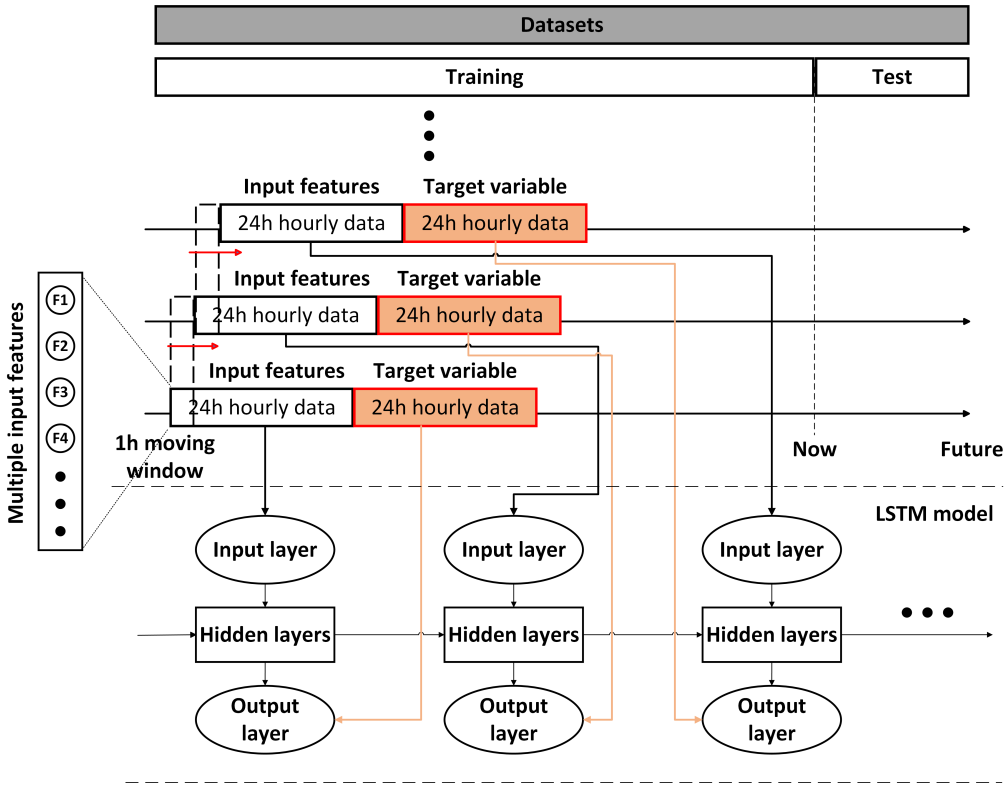

Figure 1. The proposed LSTM architecture.

3.2. The Implementation of SAA

The SAA as a centralized structure is to leverage historical and forecast data as the input variables to predict the average CIF.

We adopt methodologies similar to those used in other LSTM studies within the CIF domain. Our objective is not to outperform existing methods, but rather to examine the impact of the SDA and SAA frameworks on performance. Therefore, the feature formation aligns with established practices in the literature. As shown in Figure 2, we utilized a range

of input features, including grid electricity generation and CIF data (historical electricity generation, average CIF), grid operations and market data (historical electricity wholesale price, grid load demand, and forecast grid load demand). Historical and forecast weather variables, including wind speed, solar radiation, and precipitation, were also integrated as input features in the proposed model. These weather variables were collected at the specific geographical locations corresponding to each generator in order to capture the localized environmental conditions.

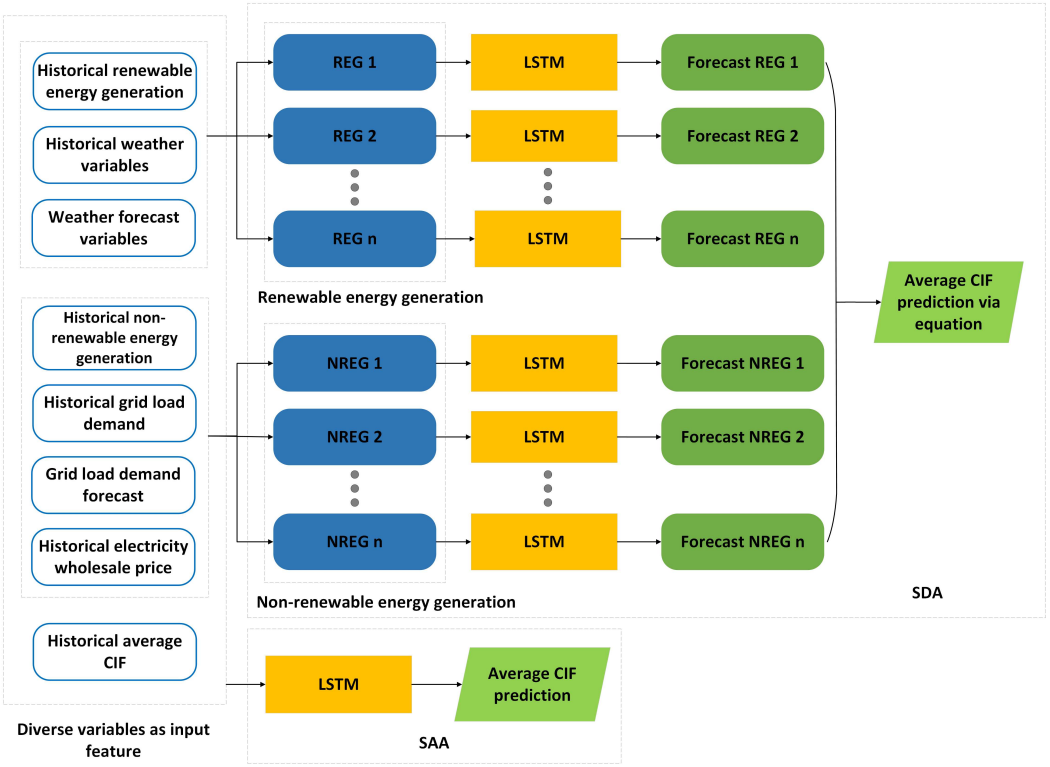

Figure 2. The diagram of SDA and SAA for average CIF prediction.

By incorporating these input features, we aimed to leverage a comprehensive range of information to improve the accuracy and robustness of our predictions. The historical average CIF and each type of energy production data provided insights into the historical patterns of carbon intensity, past performance, and trends of each source type. The grid operations and market data offered valuable information regarding the behavior of the electricity system and market dynamics. Furthermore, integrating weather variables into our model allowed us to consider the impact of weather conditions on renewable energy generation, as well as current and future electricity demand.

The 24 h historical and forecast features are collected on a daily basis. To predict the average CIF for the $(x+1)$th day, our approach involves combining the 24 h historical features from the xth day with the forecast features collected for the $(x+1)$th day. This combination of historical and forecast data enables us to capture valuable information from the past day and leverage the insights provided by the forecast for the upcoming day. By repeating this process for 24 h samples in the test set, we obtain a series of forecasts for day-ahead hourly average CIF.

3.3. The Implementation of SDA

In terms of the SDA, LSTM is employed to forecast each type of electricity generation for the following day at hourly intervals. Day-ahead average CIF prediction is calculated by aggregating each type of electricity generation forecast based on the corresponding emission factors, utilizing Equation (1). The architecture of this approach is shown in Figure 2. The correlation analysis and more advanced LSTM model are employed to enhance the

prediction accuracy of the SDA, which distinguishes our method from the original SDA proposed in [6]. Due to the varying impacts of various variables on the prediction of each type of renewable energy generation, it is crucial to carefully consider their individual influences. For instance, the wind speed directly affects the output and efficiency of wind turbines, making it a crucial factor in predicting wind power generation accurately [37]. The correlation analysis allows us to identify and understand the relationships between each variable and each type of renewable energy generation. By assessing the strength of these correlations, we can select the most influential variables for prediction. We apply the Pearson correlation coefficient (PCC) [38] to measure the correlations between available variables and different types of renewable energy generation,

$$\rho_{X,Y} = \frac{cov(X,Y)}{\sigma_X * \sigma_Y} \tag{2}$$

given a pair of variable X and renewable energy generation Y, $cov(X,Y)$ is the covariance between X and Y; σ_X and σ_Y are the standard deviations of variable X and renewable energy generation Y.

Preliminary correlation analysis between non-renewable energy generation and weather variables revealed weak relationships. Therefore, we focus solely on historical electricity wholesale prices, historical grid load demand, and forecast grid load demand as input variables for predicting non-renewable energy generation in our model. The PCC between the renewable energy generation and possible input variables are shown in Figure 3. The details and abbreviations of the input variables can be found in Section 4.1. In the range of PCC between 0 and 1, a PCC greater than 0.2 is generally interpreted as indicating a low to high positive correlation, whereas a value lower than 0.2 suggests a weak positive correlation [39]. Only the variables associated with types of renewable energy generation displaying a PCC of greater than 0.2 or lower than -0.2 are considered suitable for integration into the modeling. It is noticed that the load demand and electricity wholesale price have been identified as crucial features to predict hydro energy generation in NSW. This can be attributed to the fact that hydro energy generation integrated with storage, such as pumped hydro, can be controlled by humans based on the load demand and electricity wholesale price signals [40].

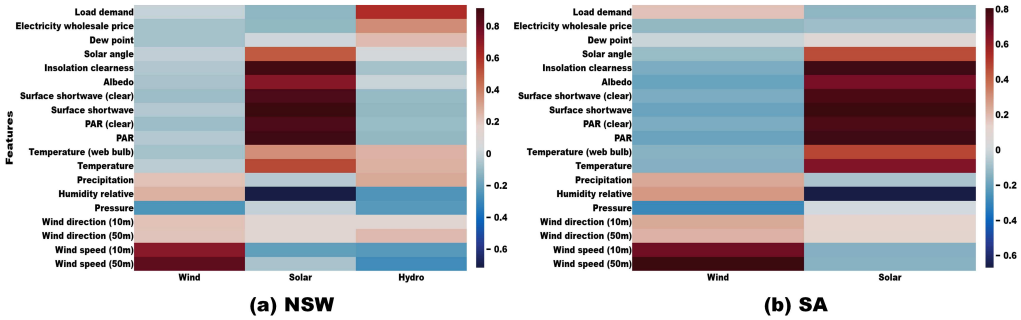

Figure 3. PCC between input features and renewable energy generation in NSW and SA.

It is worth noting that there is significant non-linearity between the variables in our studies. To address this, we also conducted a Spearman rank correlation (SRC) [41] analysis, which captures both the linear and non-linear monotonic relationships. Notably, the SRC results closely aligned with the PCC findings, indicating that the relationships between the input variables and the renewable energy generation are predominantly monotonic. This suggests that, although some non-linearities exist, they do not significantly impact the selection of key features for modeling.

4. Experiment

The data sets used in this research are first described in Section 4.1. Then, the experimental setup is presented in Section 4.2. Lastly, the experimental results and discussion are provided in Sections 4.3 and 4.4.

4.1. Data Sets

This section provides an overview of the data sets used in the study.

4.1.1. Grid Electricity Generation Data

Electricity grids across NSW and SA were considered. The proportion of electricity generation by each type of source in both areas in 2022 is presented in Figure 4. As noticed, the source and proportion of each type of renewable or non-renewable energy production are profoundly different for those two areas. NSW is a state that largely relies on non-renewable energy sources, including coal, gas combined-cycle gas turbines (CCGT), and gas open-cycle gas turbines (OCGT), which make up about 77.2% of total generation. Renewable energy sources in NSW consist of wind, solar, and hydro. In contrast, SA depends heavily on renewable energy generation, including wind and solar energy generation, which account for about 64.8% of the total generation. The non-renewable energy generation in SA comprises gas (reciprocating), gas (stream), gas CCGT, and gas OCGT technologies.

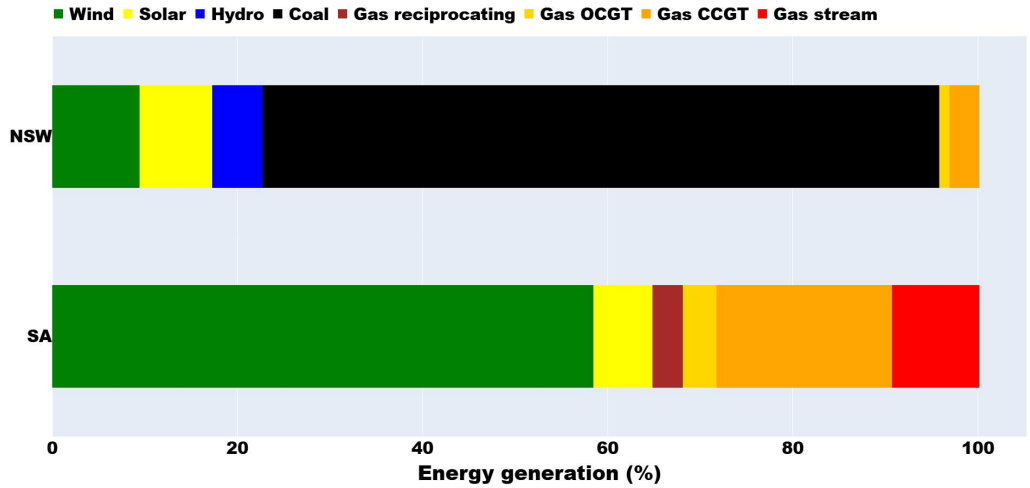

Figure 4. Different types of sources for electricity generation in NSW and SA.

For this study, electricity generation data were collected from the OpenNEM platform [42]. The data spanned a period of 2 years and were collected at 1 h intervals.

4.1.2. Weather Variable Data

The study collected historical weather variable data from the NASA POWER platform [43] and obtained forecast weather data from AccuWeather (AccuWeather for business, 2021. Available online: https://www.accuweather.com/ (accessed on 1 January 2023)). These datasets were collected at daily intervals with an hourly resolution. The weather variable data in NASA POWER is provided on a global grid with 2 to 50 m spatial resolutions based upon NASA satellite observations. Weather information at a specific location can be retrieved based on latitude and longitude input by users. Given that the openNEM platform [42] provides public access to the latitude and longitude data of all generators in Australia, it becomes feasible to acquire weather variables corresponding to the specific locations of each renewable generator across the country.

Weather variables consist of wind speed at 10 and 50 m distance range (m/s), wind direction at 10 and 50 m distance range (degree), pressure (kPa), relative humidity (%), pre-

cipitation (mm/hour), temperature (°C), wet bulb temperature (°C), sky surface shortwave downward irradiance (Wh/m^2), sky surface ultra-violet (UV) index (W/m^2), photosynthetic active radiation (PAR) index (nm), insolation clearness index (degree) and dew point (°C).

4.1.3. Grid Load Demand Data

The relationship between load demand and carbon intensity is influenced by the composition of the energy mix for electricity generation. When a substantial proportion of electricity is sourced from renewable energy with low or zero carbon emissions, the carbon intensity tends to remain relatively low, even during times of high demand. Conversely, if the energy mix relies predominantly on fossil fuel-based power plants, the carbon intensity is higher, and an increase in load demand leads to a more significant rise in carbon emissions. Hence, incorporating the load demand as an input variable in CIF forecasting is crucial. By considering the relationship between load demand and carbon intensity, the forecasting models can account for the dynamic nature of electricity consumption and its impact on carbon emissions. Both the history and forecast of hourly load demand data in Australia are provided on the Australian Energy Market Operator (AEMO) platform (Australian Energy Market Operator, 2009. Available online: https://www.aemo.com.au/ (accessed on 1 January 2023)).

4.1.4. Electricity Wholesale Price Data

The operational decision-making of generator owners and operators in Australia is significantly influenced by the wholesale electricity price. It is observed that many generators are brought online only when the market conditions are suitably beneficial, emphasizing the importance of the wholesale electricity price in shaping their operational choices. The AEMO provides reliable historical data on hourly spot prices for electricity.

4.1.5. Data Splitting

The data set comprises hourly records for a duration of two years, commencing on 2 January 2020 until 31 December 2021, for each geographical region. We use the first year of data (2 January 2020 to 1 January 2021, inclusive) to train the SDA and SAA models, and then test the performance of these models on the following year of data (2 January 2021 to 31 December 2021, inclusive).

4.2. Experimental Setup

4.2.1. Evaluation Metric

MAPE, defined by Equation (3), is a common metric to evaluate the accuracy of time series forecasting [44]. It is used to measure the accuracy of a forecasting model by calculating the average percentage difference between the predicted values and the actual values.

$$MAPE = \frac{1}{n}\sum_{i=1}^{n}\left|\frac{A_i - F_i}{A_i}\right| * 100 \quad (3)$$

where n is the number of observations, and A_i and F_i are the actual and forecast values at sample i.

Mean Absolute Error (MAE) is a widely used performance metric in machine learning and statistical analysis, quantifying the average deviation between predicted and actual data [45]. It is calculated as the average of the absolute differences between predicted and actual values, as shown in Equation (4). Certain energy sources, such as solar and gas power production, often yield zero values. Consequently, using MAPE as an evaluation metric is impractical in these cases, as it does not produce meaningful results. Therefore, MAE is a more suitable alternative for evaluating the forecasting performance of each individual energy type in the SDA.

$$MAE = \frac{1}{n}\sum_{i=1}^{n}|A_i - F_i| \quad (4)$$

In this research, the standard deviation is utilized to assess the statistical significance of the results, enabling us to derive meaningful insights.

$$\sigma = \sqrt{\frac{1}{n}\sum_{i=1}^{n}(x_i - \mu)^2} \quad (5)$$

where x_i is the ith observation, and μ is the mean of all of the observations.

4.2.2. LSTM Model Setup

The LSTM model was applied separately to forecast (1) the individual energy type production for the SDA, and (2) the average CIF for the SAA, with encoding and decoding structure. The input features were discussed in Section 4.1.

The hyperparameters for the model were selected through a grid-search over the parameters shown in Table 1. We built the models with two LSTM layers (200 nodes each) and one dense layer for both methods with a batch size of 64. The dropout function was applied to avoid overfitting, and settled at 0.5. For the SDA, the learning rate and epoch were experimentally determined to be 0.0004 and 300–600, depending on the different sources. For the SAA, we empirically set the learning rate and epoch to be 0.0004 and 800.

Table 1. Details of hyperparameters for the LSTM model optimized by grid-search.

Hyperparameters	Ranges
Epochs	200, 300, 400, 500, 600, 700, 800, 900
Batch Size	32, 64, 128
Learning Rate	0.0002, 0.0004, 0.0006
Number of Layers	1, 2, 3, 4, 5
Units per Layer	150, 200, 250
Dropout Rate	0.4, 0.5, 0.6
Activation	relu, tanh
Optimizer	Adam, RMSprop
Loss Function	RMSE, MAE
Normalization	MinMaxScaler, StandardScaler

The "EarlyStopping" method was used to terminate training once the performance of model stopped continually improving. The Root Mean Squared Error (RMSE) loss function was applied to evaluate the training loss. The "Adam" optimization function and the "ReLu" activation function were considered in the model building. We applied the "MinMaxScaler" normalization function as the pre-processing and post-processing steps to reduce variance relatively and maintain the stability of the features. Further, the sliding-window technique was used with prior 24 h time steps to predict the next 24 h time steps, as shown in Figure 1.

4.3. Experimental Results

To evaluate the performance of both approaches, this study first compared their general performance in NSW and SA. Next, the performance of both approaches was assessed under different levels of stochastic renewable energy generation compared to more predictable base-load (fossil-fueled) energy generation in those two regions. This evaluation reflects real-world conditions where renewable energy sources are increasingly integrated into the grid. Furthermore, both approaches were compared under controlled and curtailed generation scenarios regulated by the grid, which tests the adaptability of the algorithms to regulatory constraints. Lastly, the generation prediction performance of the SDA was evaluated to identify gaps in its forecasting capabilities, highlighting areas for improvement in predictive accuracy essential for grid management and energy planning.

4.3.1. Overall Performance

An overall comparison experiment was conducted to examine the general performance of both approaches in NSW and SA. The MAPE and MAE of the average CIF forecasting in NSW and SA using each approach is displayed in Table 2. Both proposed approaches have shown higher accuracy in NSW. As illustrated in Figure 4, the proportion of renewable energy generation in SA surpasses that of NSW by a significant margin. The observed discrepancy indicates that in scenarios with a higher proportion of renewable energy generation, the errors of both approaches are prone to increasing. This can be attributed to the unpredictable and dynamic nature of renewable energy generation, which is influenced by factors such as weather conditions, electricity wholesale prices, and grid load demand. These variables significantly impact the individual production of renewable sources, leading to their volatile and fluctuating behavior. In contrast, non-renewable energy generation, such as coal, is more predictable because it is generally controlled by humans and the fluctuation of non-renewable energy generation is relatively stable.

Table 2. The MAPE and MAE of average CIF forecasting in different states using two approaches.

State	MAPE (%)		MAE	
	SAA	**SDA**	**SAA**	**SDA**
NSW	5.40	5.22	0.037	0.036
SA	26.71	27.76	0.049	0.050

The four best cases where one approach outperforms the other in terms of accuracy for a single day in both NSW and SA are shown in Figure 5. The blue, red, and orange lines represent the actual CIF, the forecast from the SAA, and the forecast from the SDA, respectively. It can be observed that the actual CIF in SA exhibits lower levels compared with NSW. Upon analyzing the energy profiles and CIF patterns, it becomes evident that the actual CIF pattern in NSW exhibits a higher degree of regularity compared to that observed in SA. This heightened regularity translates to increased predictability in the CIF forecasting, which results in both approaches achieving a better performance in NSW. Regardless of the cases one approach outperforms the other according to MAPE, we observe that in these cases, SDA forecasts track the trend of the actual carbon intensity over time.

4.3.2. Analyzing Performance across Different Scenarios

It is helpful to uncover the scenarios that give rise to the superiority of one approach over the other under real-world conditions.

The performance of each approach in relation to the range of magnitudes for the features can vary. There is no definitive threshold or level at which one approach outperforms the other. Therefore, it is important to evaluate the performance of both approaches across different ranges of feature magnitudes to examine which approach performs better in a given context. We defined a metric as follows in Equation (6) to gain insights into this difference.

$$\Delta Mi = M_A i - M_D i \tag{6}$$

where $M_A i$ and $M_D i$ denote the MAPE of SAA and SDA in predicting CIF at sample i. The difference in MAPE between both approaches, denoted as ΔMi, is calculated. If ΔMi yields a negative value, it indicates that the SAA outperforms the SDA for sample i. Conversely, a positive ΔMi signifies that the SDA outperforms the SAA.

We analyze both typical and atypical scenarios to uncover and understand the differences between these two approaches. Typical scenarios refer to the CIF forecasts of both approaches under standard grid power conditions, while atypical scenarios involve their forecasts during interventions.

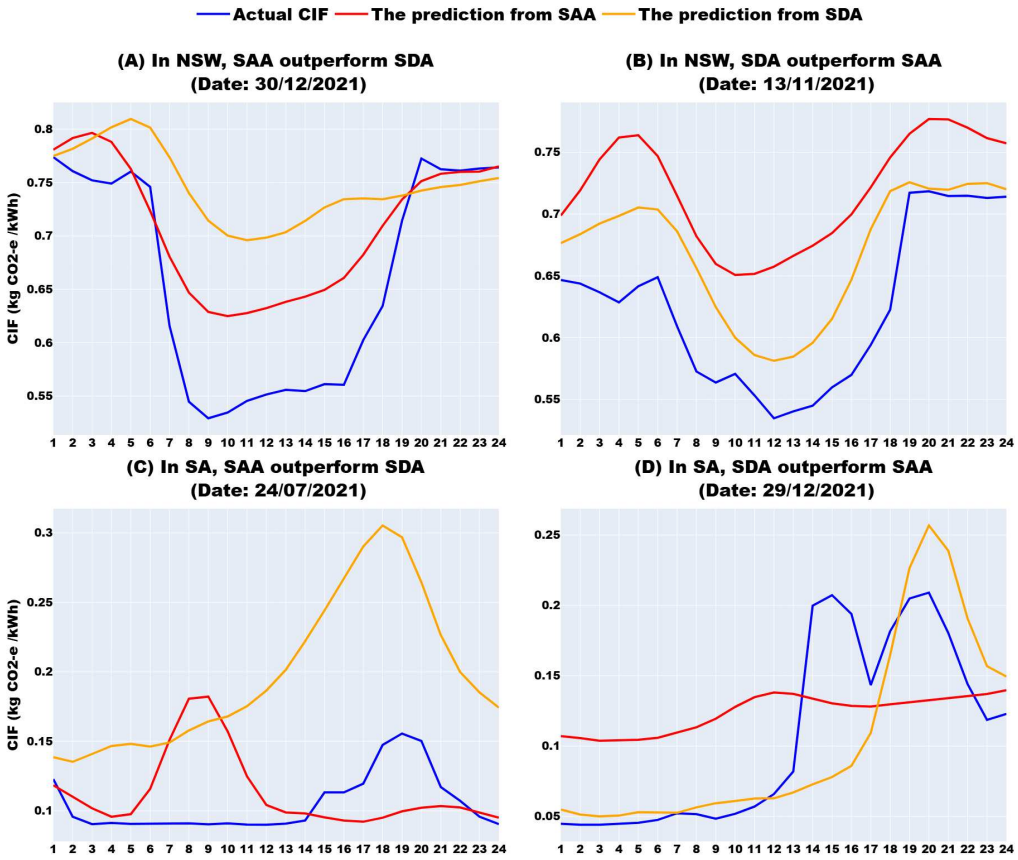

Figure 5. The four best cases where one approach outperforms the other in terms of accuracy for a single day in two states.

Typical Scenarios

We aim to understand which feature differences lead to the sharpest difference in performance between SDA and SAA. To achieve this, we first identify the time periods where the performance differences are most significant and then examine the characteristics of the input features during those periods. Specifically, the extreme cases were selected as the samples, the corresponding ΔMi values of which are among the largest or smallest 2.5% across all of the samples. Within these extreme cases, we calculated the average magnitudes of the corresponding features. In order to standardize the results and ensure comparability, we employed Min–Max normalization [46] to scale the values between 0 and 1, facilitating further analysis.

All features mentioned in Section 4.1 used by both approaches are analyzed, as shown in Figure 6. The yellow blocks highlight the distinct differences in feature magnitudes between the two approaches. SDA is superior in NSW when wind and hydro energy generation (and related weather predictors, e.g., wind speed and relative humidity) are high. In contrast, the SAA is found to be more accurate when solar energy generation (and related predictors, e.g., PAR and surface shortwave) are high. SDA is superior in SA when solar energy generation is high. In contrast, SAA is found to be more accurate when wind generation is high and also when overall load demand is high.

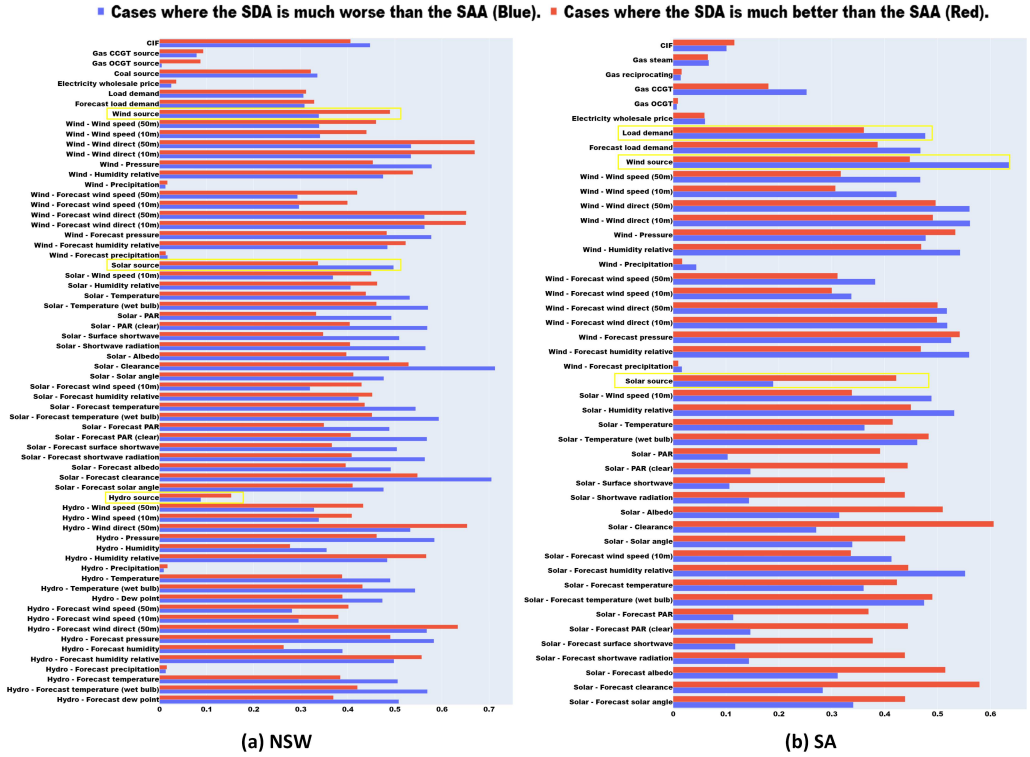

Figure 6. The normalized magnitude of each feature for the extreme cases.

Furthermore, we examined the proportion of renewable energy generation in the extreme cases previously defined, as shown in Figure 7. It is observed that in the cases where the SAA outperforms the SDA in NSW, solar energy generation accounts for 16.42% of the total generation, surpassing other renewable source types. In SA, wind energy generation constitutes 76% of the total generation in the same scenario as noticed in Figure 7b. In NSW, the SAA outperforms the SDA when solar power is the primary source of renewable energy. In SA, the SAA performs better when wind power is the dominant source of renewable energy. These findings are consistent with the aforementioned empirical results, and demonstrate that the SAA yields more accurate predictions in the presence of dominant renewable energy generation. However, the performance of SAA tends to decline compared to the SDA approach when niche renewable energy generation types produce higher outputs than usual. For instance, situations with elevated niche renewable energy generation, such as wind and hydro energy generation in NSW, typically dominated by solar energy generation, and solar energy generation in SA, traditionally reliant on wind power, can lead to a degradation in SAA performance.

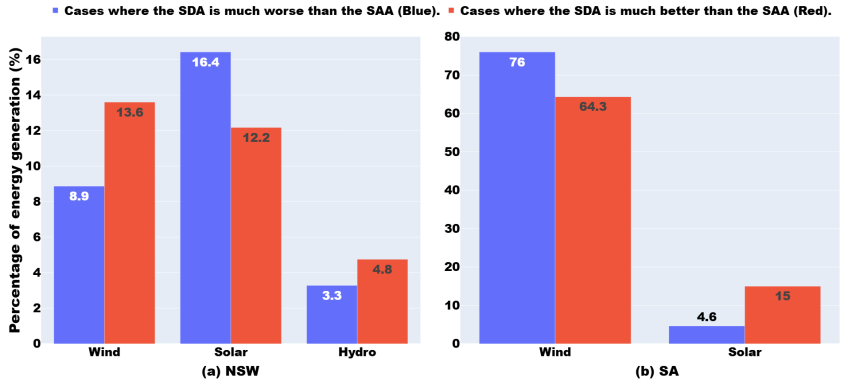

Figure 7. The penetration of each renewable energy generation for the extreme cases.

The difference in the grid load demand between the two extreme cases in NSW is negligible, as demonstrated in Figure 6a. This can be attributed to the marginal difference in coal electricity production, which is the primary source type of energy generation in NSW. However, wind energy holds the largest share of electricity supply in SA. As noticed in Figure 6b, the proposed SAA exhibits better performance even under higher load demands.

Based on the analysis, it is recommended to prioritize the use of SAA when the dominant source of renewable energy generation is higher, and to use SDA more when the non-dominant source is higher. For example, if a user is deciding between SAA and SDA and expects more windy weather in a wind-dominant energy region in the coming days, we advise choosing SAA for CIF forecasting. Conversely, if an increase in solar radiation and less wind are anticipated in the same region, SDA should be preferred for more accurate forecasts.

Atypical Scenarios

While electricity generation from solar and wind is primarily influenced by weather variables, it may also be influenced (though less typically) by human intervention (e.g., the decision to redirect renewable output to onsite storage during periods of low wholesale price or to curtail generation during negative price events). This motivates us to evaluate which approach is better suited for predicting CIF when atypical scenarios like human intervention arise in renewable energy generation. These scenarios, particularly human intervention, may include redirecting renewable outputs to charge on-site battery systems or implementing generation curtailment during periods of negative or low wholesale prices. Firstly, we conducted a filtering process to identify highly correlated features for each type of renewable energy generation in both regions. Secondly, we calculated the PCC between the types of renewable energy generation and their corresponding selected features, specifically focusing on cases where one approach significantly outperforms the other. Finally, the difference in PCC for each type of renewable energy generation between the two approaches provides insights into the differing degrees of human interventions involved in each approach.

Most of the time, a small set of variables are highly predictive of the outputs of each generator. As shown in Figure 8, based on the PCC, wind speed is unsurprisingly highly correlated with wind generation, a set of solar irradiance and temperature variables are highly correlated with solar generation, and load demand is relatively predictive of hydro generation. However, to what extent does each framework rely on these strong correlations holding? To explore this, we examined situations where SDA performs much worse or much better than SAA in each state, focusing on how the average of PCC values for the key predictors of each generation type (all variables to the right of the red dashed line in Figure 8) relate to the performance of each framework. It is consistently the case that SDA performs worst when outputs are less well correlated with the typical predictors of the outputs of each generator, as shown in Figure 9. This likely reflects times when the output of one generation source is impacted by broader grid dynamics. For instance, high wind conditions may become uncorrelated with wind outputs if an excess supply of solar energy and low load demand significantly drive down prices, prompting operators to redirect generation to onsite batteries or, in extreme cases, curtail output. Without explicitly integrating variables associated with other generation sources, the individual outputs from SDA are likely to falter in these instances, leading to lower accuracy in CIF outputs. This is not an issue with SAA, which includes all available input variables and can therefore better learn cross-generation relationships.

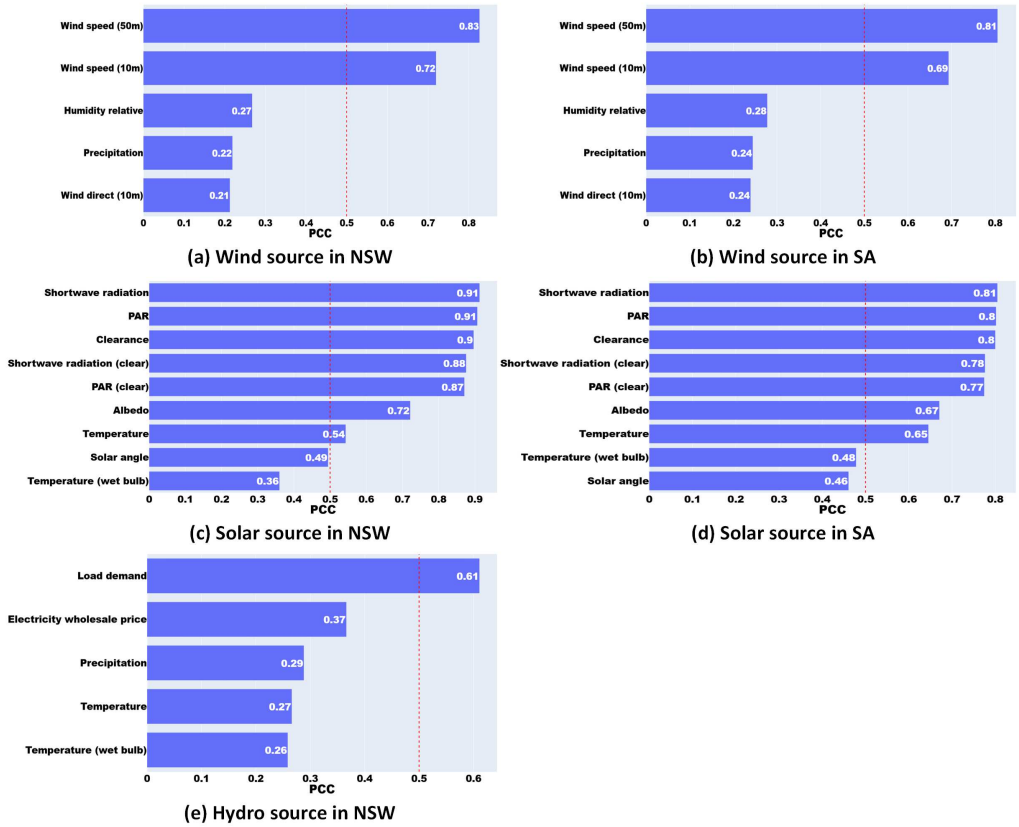

Figure 8. The PCC between different types of renewable energy generation and their relevant features based on all samples in NSW and SA.

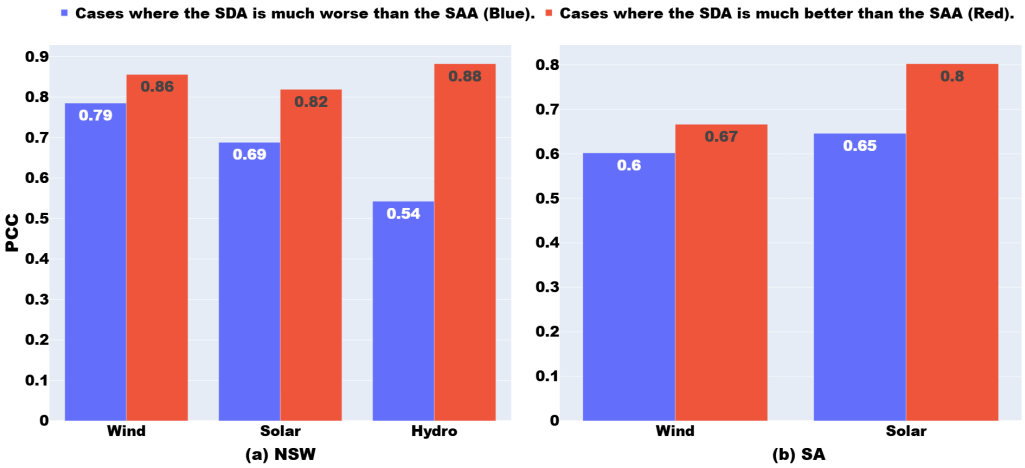

Figure 9. The PCC between different types of renewable energy generation and their highly relevant features for the extreme cases in NSW and SA.

4.3.3. How to Improve the SDA

The performance of the SDA is determined by the result of each type of electricity generation prediction. Consequently, the error derived from renewable and non-renewable energy generation forecasts in the SDA can be analyzed to assess the impact of each category of electricity production forecasting on CIF forecasting. To compare the prediction performance of both approaches, we employed Equation (6) to calculate ΔMi similarly. The extreme cases were chosen as samples based on the largest or smallest 2.5% of the corresponding ΔMi values across all the samples. The MAPE values of the renewable and

non-renewable energy generation forecasts obtained using the SDA are analyzed using the method described, and results depicted in Figure 10. The analysis indicates that renewable energy generation forecasting presents a markedly greater difference between the extreme cases of CIF forecasting performance in NSW when compared with non-renewable energy generation forecasting. Conversely, a noticeable difference between the extreme cases can be observed when evaluating non-renewable energy generation predictions in SA. As noted in Figure 4, the NSW depends heavily on non-renewable energy generation, while the SA relies more on renewable energy generation. The results indicate that the SDA could be further developed through improving the power generation prediction performance of the types that accounts for a lower penetration in a specific area.

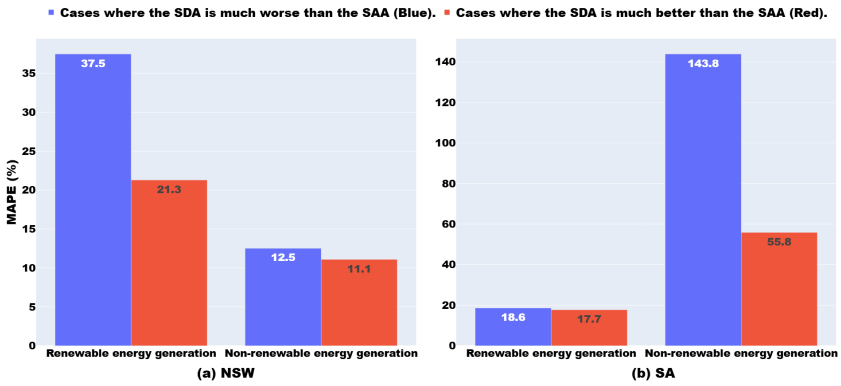

Figure 10. The MAPE of renewable and non-renewable energy generation forecasting for the extreme cases.

Moreover, we analyzed the individual prediction impacts of different renewable energy generation types in NSW and non-renewable energy generation types in SA on CIF forecasting. The MAE of each type of renewable energy generation forecast in NSW and non-renewable energy generation forecast in SA, as determined by the ranking method used previously and the selection of 2.5% extreme cases, is presented in Figure 11. The substantial variation in solar energy generation forecasting performance between the two extreme cases in NSW provides valuable insight into the potential benefits of enhancing predictive accuracy for areas with low penetration of renewable energy generation. Similarly, in SA, all forecasts of gas-power production, including gas OCGT, gas CCGT, gas reciprocating, and gas steam, display a noticeable distinction in this analysis, highlighting the potential for further improvement.

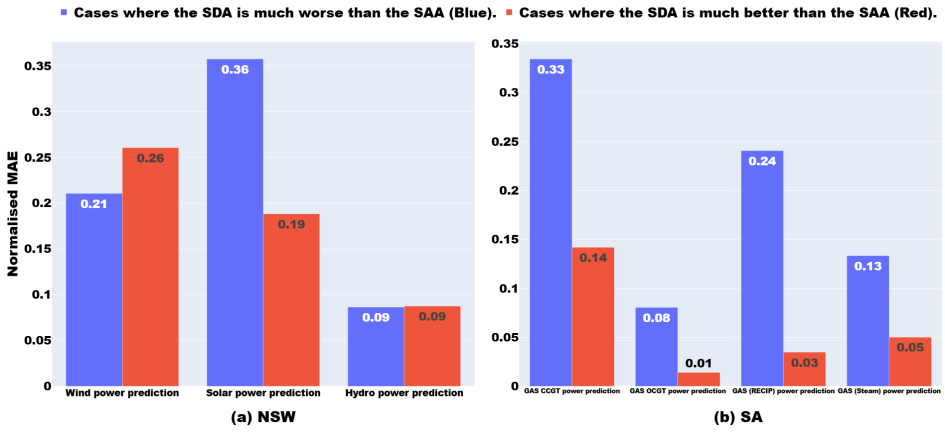

Figure 11. The normalized MAE of different types of energy generation forecasting for the extreme cases.

Forecasting energy generation with SDA is challenging due to periods of complete inactivity, variable peaking output, and the infrequent activation of energy sources. Forecasting solar power generation may be difficult during the day in cloudy conditions where minimal (but non-zero) levels of irradiance are experienced. In addition, the limited presence of non-renewable energy generation in the energy mix of SA leads to gas-related energy generation being activated infrequently and primarily in response to price signals. Gas energy generation in SA features a range of outputs, with some plants (e.g., gas steam and gas CCGT) providing variable, responsive power for both base and peak loads, while others (e.g., gas reciprocating engines and gas OCGT) operate intermittently during peak demand. Accurately forecasting solar and gas power generation is challenging, especially during periods of extremely low and consistent generation rates, along with the infrequent activation of gas-peaking plants. These challenges contribute significantly to sub-optimal energy generation forecasts. The SDA often encounters difficulties in effectively training for electricity generation during daily operations, particularly in scenarios with extremely low penetration levels of energy generation that operate at or near zero values and inconsistent values, such as during periods of outage or ramping up. Additionally, SDA would find it challenging to forecast intermittently peaking energy generation, such as gas plants transitioning from inactive to high generation levels.

4.4. Discussion

The comparison reveals that both approaches achieve comparable accuracy in forecasting CIF, with overall comparable performance. Both approaches demonstrate significantly enhanced performance in predicting CIF for NSW, characterized by fossil-fuel-dominated regions, as compared to SA, with more stochastic renewable energy generation. The SAA exhibits superior performance when the generation of dominant renewable energy is higher, but its performance is reduced during periods of increased niche energy generation types compared to the SDA. Renewable source types are projected to be the primary sources for meeting electricity demand in the coming decades, with increased penetration of dominant renewable energy generation. Furthermore, the comparative results demonstrate the effectiveness of the SAA in cases where renewable energy generation is subject to atypical scenarios, such as human interventions and regular controls. It is common for renewable energy generation to be controlled or curtailed under certain circumstances to ensure engine safety and address negative or low wholesale price scenarios. The SAA can account for the interrelationships between source types, resulting in improved CIF forecasting performance. The SDA exhibits limitations in accurately predicting consistent generation from certain source types, particularly those with extremely low production magnitudes and steady values, as well as when deviations from typical conditions occur, such as the activation of a peaking plant.

In light of the characteristics of both approaches, we offer some recommendations for improvement. Given the inability of the SDA to accurately predict consistent generation from some source types, particularly those with extremely low production magnitudes and consistent values, it is crucial to first employ an approach, such as incorporating expert knowledge, to identify whether a source type is operational or shut down before conducting generation prediction. This will enhance the prediction accuracy for each source type and, thus, the final CIF. Additionally, addressing "zero-output" times can be achieved by incorporating basic heuristics, such as zeroing-out time periods overnight for solar generation. Moreover, when predicting energy generation, we can explore the integration of heuristics to account for human interventions or grid curtailment scenarios. In terms of SAA, the performance of the SAA appears to be weaker during periods of atypical behavior, such as an increase in more niche generation types. To improve performance during such atypical times, a more careful selection of training data that balances fuel-mix types and operational scenarios may be beneficial. Improving the model interpretability of the SAA can be achieved through several approaches, such as sensitivity analysis and expert feedback. Including high-quality electricity wholesale price forecasts potentially

enhance the accuracy of both approaches. Wholesale price forecasts have a significant influence on the operation of non-baseload generation, as their operations are strongly guided by market incentives. In addition, wholesale price forecasts offer valuable insights into the impact of market incentives on CIF patterns in earlier times, enabling the forecast of SAA to align with the anticipation of peak and off-peak periods in the CIF.

5. Conclusions

In this study, both SAA and SDA were examined for day-ahead grid average CIF prediction. The SAA and SDA are separately structured as centralization and distribution designs. This study aims to identify under what conditions and for what reasons one approach outperforms the other while also offering guidance for improving the approach that exhibits weaknesses.

The comparison between the SAA and SDA forecasting methods shows that both achieve similar accuracy in predicting CIF, particularly excelling in fossil-fuel-heavy regions like NSW, compared to the more variable renewable energies of SA. The SAA performs better with dominant renewable energy sources, but less effectively with niche types. It is effective in scenarios where renewable generation is adjusted for safety or pricing concerns, reflecting the interplay between different energy sources. In contrast, the SDA struggles to consistently predict outputs from sources with very low or uniform production levels.

To enhance CIF forecasting accuracy with the SDA, it is recommended to validate the operational status of energy sources before making predictions. Implementing simple heuristics, such as turning off solar power overnight, could improve accuracy. Additionally, factoring in human interventions or grid curtailments may be beneficial. For the SAA, optimizing the training dataset to balance different fuel types and operational conditions during unusual activity could improve performance. Also, enhancing SAA interpretability through sensitivity analysis and expert input, alongside incorporating detailed electricity wholesale price forecasts, could align predictions more closely with market trends.

For future research, it would be beneficial to include a broader range of regions beyond NSW and SA and utilize larger datasets encompassing multiple years to further consolidate the findings.

Author Contributions: Conceptualization, B.Z., H.T., A.B., H.H. and A.C.R.; methodology, B.Z., H.T., A.B., H.H. and A.C.R.; software, B.Z.; validation, B.Z., H.T. and A.B.; formal analysis, B.Z., H.T., A.B., H.H. and A.C.R.; investigation, B.Z., H.T., A.B., H.H. and A.C.R.; data curation, B.Z. and H.H.; writing—original draft preparation, B.Z.; writing—review and editing, B.Z., H.T., A.B., H.H. and A.C.R.; visualization, B.Z.; supervision, H.T., A.B., H.H. and A.C.R.; project administration, H.H. and A.C.R.; funding acquisition, A.B. and A.C.R. All authors have read and agreed to the published version of the manuscript.

Funding: This study received funding from the RACE for 2030 Cooperative Research Centre, with support from Buildings Alive Pty Ltd and the University of Technology Sydney.

Institutional Review Board Statement: Not applicable.

Informed Consent Statement: Not applicable.

Data Availability Statement: Data are contained within the article.

Conflicts of Interest: Author A. Craig Roussac has an ongoing role with Buildings Alive Pty Ltd., and author Hao Huang was previously employed by the company. The remaining authors declare that the research was conducted in the absence of any commercial or financial relationships that could be construed as a potential conflicts of interest. The authors declare that this study received funding from the RACE for 2030 Cooperative Research Centre, with support from Buildings Alive Pty Ltd. and the University of Technology Sydney, which provided a PhD scholarship for this research.

References

1. Intergovernmental Panel on Climate Change (IPCC). Global Warming of 1.5 °C. 2018. Available online: https://www.ipcc.ch/sr15 (accessed on 1 January 2023).
2. International Energy Agency (IEA). CO_2 Emissions in 2022. 2023. Available online: https://www.iea.org/reports/CO2-emissions-in-2022 (accessed on 10 September 2024).
3. United Nations Environment Programme. Paris Agreement. 2015. Available online: https://wedocs.unep.org/20.500.11822/20830 (accessed on 1 January 2023).
4. den Elzen, M.G.; Dafnomilis, I.; Forsell, N.; Fragkos, P.; Fragkiadakis, K.; Höhne, N.; Kuramochi, T.; Nascimento, L.; Roelfsema, M.; van Soest, H.; et al. Updated nationally determined contributions collectively raise ambition levels but need strengthening further to keep Paris goals within reach. *Mitig. Adapt. Strateg. Glob. Chang.* **2022**, *27*, 33. [CrossRef] [PubMed]
5. Dincer, I. Renewable energy and sustainable development: A crucial review. *Renew. Sustain. Energy Rev.* **2000**, *4*, 157–175. [CrossRef]
6. Maji, D.; Sitaraman, R.K.; Shenoy, P. DACF: Day-ahead carbon intensity forecasting of power grids using machine learning. In Proceedings of the Thirteenth ACM International Conference on Future Energy Systems, Virtual, 28 June–1 July 2022; pp. 188–192. [CrossRef]
7. Maji, D.; Shenoy, P.; Sitaraman, R.K. Multi-day forecasting of electric grid carbon intensity using machine learning. *ACM SIGENERGY Energy Inform. Rev.* **2023**, *3*, 19–33. [CrossRef]
8. Lowry, G. Day-ahead forecasting of grid carbon intensity in support of HVAC plant demand response decision-making to reduce carbon emissions. *Build. Serv. Eng. Res. Technol.* **2018**, *39*, 749–760. [CrossRef]
9. Leerbeck, K.; Bacher, P.; Junker, R.G.; Goranović, G.; Corradi, O.; Ebrahimy, R.; Tveit, A.; Madsen, H. Short-term forecasting of CO_2 emission intensity in power grids by machine learning. *Appl. Energy* **2020**, *277*, 115527. [CrossRef]
10. Bokde, N.D.; Tranberg, B.; Andresen, G.B. Short-term CO_2 emissions forecasting based on decomposition approaches and its impact on electricity market scheduling. *Appl. Energy* **2021**, *281*, 116061. [CrossRef]
11. Aryai, V.; Goldsworthy, M. Day ahead carbon emission forecasting of the regional National Electricity Market using machine learning methods. *Eng. Appl. Artif. Intell.* **2023**, *123*, 106314. [CrossRef]
12. Zhang, X.; Wang, D. A GNN-based Day Ahead Carbon Intensity Forecasting Model for Cross-Border Power Grids. In Proceedings of the 14th ACM International Conference on Future Energy Systems, Orlando, FL, USA, 20–23 June 2023; pp. 361–373. [CrossRef]
13. Riekstin, A.C.; Langevin, A.; Dandres, T.; Gagnon, G.; Cheriet, M. Time Series-Based GHG Emissions Prediction for Smart Homes. *IEEE Trans. Sustain. Comput.* **2018**, *5*, 134–146. [CrossRef]
14. Peng, B.; Li, Y.; Yang, C.; Feng, H.; Gong, X.; Liu, Z.; Zhong, J.; Huan, J. Probabilistic grid carbon intensity forecasting with Hodrick–Prescott decomposition. *Energy Rep.* **2024**, *11*, 5400–5406. [CrossRef]
15. Cai, M.; Huang, L.; Zhang, Y.; Liu, C.; Li, C. Day-Ahead Forecast of Carbon Emission Factor Based on Long and Short-Term Memory Networks. In Proceedings of the 2023 5th Asia Energy and Electrical Engineering Symposium (AEEES), Chengdu, China, 23–26 March 2023; pp. 1568–1573. [CrossRef]
16. Santos, T.; Bessani, M.; da Silva, I. Evolving Dynamic Bayesian Networks for CO_2 Emissions Forecasting in Multi-Source Power Generation Systems. *IEEE Lat. Am. Trans.* **2023**, *21*, 1022–1031. [CrossRef]
17. Ostermann, A.; Bajrami, A.; Bogensperger, A. Short-term forecasting of German generation-based CO_2 emission factors using parametric and non-parametric time series models. *Energy Inform.* **2024**, *7*, 2. [CrossRef]
18. Baker, P.; Mitchell, C.; Woodman, B. Electricity market design for a low-carbon future. *UKERC* **2010**, *24*. Available online: https://ukerc.ac.uk/publications/electricity-market-design-for-a-low-carbon-future/ (accessed on 1 January 2023).
19. Yang, J.; Zhao, J.; Luo, F.; Wen, F.; Dong, Z.Y. Decision-Making for Electricity Retailers: A Brief Survey. *IEEE Trans. Smart Grid* **2017**, *9*, 4140–4153. [CrossRef]
20. Lim, B.; Zohren, S. Time-series forecasting with deep learning: A survey. *Philos. Trans. R. Soc. A* **2021**, *379*, 20200209. [CrossRef]
21. Hochreiter, S.; Schmidhuber, J. Long Short-Term Memory. *Neural Comput.* **1997**, *9*, 1735–1780. [CrossRef]
22. Finenko, A.; Cheah, L. Temporal CO_2 emissions associated with electricity generation: Case study of Singapore. *Energy Policy* **2016**, *93*, 70–79. [CrossRef]
23. Mason, K.; Duggan, J.; Howley, E. Forecasting energy demand, wind generation and carbon dioxide emissions in Ireland using evolutionary neural networks. *Energy* **2018**, *155*, 705–720. [CrossRef]
24. Linardatos, P.; Papastefanopoulos, V.; Panagiotakopoulos, T.; Kotsiantis, S. CO_2 concentration forecasting in smart cities using a hybrid ARIMA–TFT model on multivariate time series IoT data. *Sci. Rep. Nat.* **2023**, *13*, 17266. [CrossRef]
25. Han, Z.; Cui, B.; Xu, L.; Wang, J.; Guo, Z. Coupling LSTM and CNN neural networks for accurate carbon emission prediction in 30 Chinese provinces. *Sustainability* **2023**, *15*, 13934. [CrossRef]
26. Yuan, H.; Ma, X.; Ma, M.; Ma, J. Hybrid framework combining grey system model with Gaussian process and STL for CO_2 emissions forecasting in developed countries. *Appl. Energy* **2024**, *360*, 122824. [CrossRef]
27. Li, Y.; Wang, Z.; Liu, S. Enhance carbon emission prediction using bidirectional long short-term memory model based on text-based and data-driven multimodal information fusion. *J. Clean. Prod.* **2024**, *471*, 143301. [CrossRef]
28. Gu, H.; Wu, L. Pulse fractional grey model application in forecasting global carbon emission. *Appl. Energy* **2024**, *358*, 122638. [CrossRef]

29. Chen, J.; Gerbig, C.; Marshall, J.; Totsche, K.U. Short-term forecasting of regional biospheric CO_2 fluxes in Europe using a light-use-efficiency model. *Geosci. Model Dev. Discuss.* **2019**, *2019*, 1–26. [CrossRef]
30. Çiğdem Köne, A.; Büke, T. Forecasting of CO_2 emissions from fuel combustion using trend analysis. *Renew. Sustain. Energy Rev.* **2010**, *14*, 2906–2915. [CrossRef]
31. Regett, A.; Böing, F.; Conrad, J.; Fattler, S.; Kranner, C. Emission Assessment of Electricity: Mix vs. Marginal Power Plant Method. In Proceedings of the 2018 15th International Conference on the European Energy Market (EEM), Lodz, Poland, 27–29 June 2018; pp. 1–5. [CrossRef]
32. Hawkes, A.D. Estimating marginal CO_2 emissions rates for national electricity systems. *Energy Policy* **2010**, *38*, 5977–5987. [CrossRef]
33. International Energy Agency (IEA). *CO_2 Emissions from Fuel Combustion*; Organization for Economic: France, Paris, 2012. [CrossRef]
34. Torres, J.F.; Hadjout, D.; Sebaa, A.; Martínez-Álvarez, F.; Troncoso, A. Deep learning for time series forecasting: A survey. *Big Data* **2021**, *9*, 3–21. [CrossRef]
35. Merity, S.; Keskar, N.S.; Socher, R. Regularizing and optimizing LSTM language models. *arXiv* **2017**, arXiv:1708.02182.
36. Ying, X. An overview of overfitting and its solutions. *J. Phys. Conf. Ser.* **2019**, *1168*, 022022.
37. Gao, Y.; Billinton, R. Adequacy assessment of generating systems containing wind power considering wind speed correlation. *IET Renew. Power Gener.* **2009**, *3*, 217–226. [CrossRef]
38. Pearson, K. VII. Mathematical contributions to the theory of evolution.—III. Regression, heredity, and panmixia. *Philos. Trans. R. Soc. Lond. Ser. A* **1896**, *187*, 253–318. [CrossRef]
39. Schober, P.; Boer, C.; Schwarte, L.A. Correlation Coefficients: Appropriate Use and Interpretation. *Anesth. Analg.* **2018**, *126*, 1763–1768. [CrossRef] [PubMed]
40. Barbour, E.; Wilson, I.G.; Radcliffe, J.; Ding, Y.; Li, Y. A review of pumped hydro energy storage development in significant international electricity markets. *Renew. Sustain. Energy Rev.* **2016**, *61*, 421–432. [CrossRef]
41. Zar, J.H. Spearman Rank Correlation. *Encycl. Biostat.* **2005**, *7*. [CrossRef]
42. Dylan, M.; Simon, H.C.; Steven, T.; Nik, C. An Open Platform for National Electricity Market Data. 2022. Available online: https://opennem.org.au/ (accessed on 1 January 2023).
43. The NASA POWER Team. Prediction of Worldwide Energy Resources (POWER) Project. 2021. Available online: https://power.larc.nasa.gov/data-access-viewer/ (accessed on 1 January 2023).
44. Benidis, K.; Rangapuram, S.S.; Flunkert, V.; Wang, Y.; Maddix, D.; Turkmen, C.; Gasthaus, J.; Bohlke-Schneider, M.; Salinas, D.; Stella, L.; et al. Deep learning for time series forecasting: Tutorial and literature survey. *ACM Comput. Surv.* **2022**, *55*, 1–36. [CrossRef]
45. Willmott, C.J.; Matsuura, K. Advantages of the mean absolute error (MAE) over the root mean square error (RMSE) in assessing average model performance. *Clim. Res.* **2005**, *30*, 79–82. [CrossRef]
46. Han, J.; Kamber, M.; Pei, J. Data mining concepts and techniques third edition. In *University of Illinois at Urbana-Champaign Micheline Kamber Jian Pei Simon Fraser University*; Morgan Kaufmann: Burlington, MA, USA, 2012. [CrossRef]